Synthesis and Structure of Boron Compounds Bearing Tridentate Ligands with 1,3-Bicarbonylbenzene Skeleton

Jun-ya Nakatsuji and Yohsuke Yamamoto*

Department of Chemistry, Graduate School of Science, Hiroshima University,
1-3-1 Kagamiyama, Higashi-Hiroshima 739-8526

Received December 24, 2009; E-mail: yyama@sci.hiroshima-u.ac.jp

In order to examine differences in structure due to the electronic nature of the oxygen ligand, several organoboron compounds bearing ester **8a**–**8c** and amide **13a** and **13b** ligands were prepared and crystallographically analyzed. In the ester ligand systems, the pinacolato derivative **8a** and catecholato derivative **8b** took a pentacoordinate structure, while fluorenyl derivative **8c** took a tetracoordinate structure instead of pentacoordinate due to the strong electrophilic nature of the boron atom. In contrast to the ester ligand systems, no pentacoordinate species were found in the amide ligand systems. The pinacolato derivative **13a** is tricoordinated, and catecholato derivative **13b** is tetracoordinated. These results could be due to the steric effect of the diisopropylamide ligand together with the electronic effects. The VT NMR study and the DFT calculations reveal that the energy difference between the tetracoordinate and pentacoordinate structure in **8c** is very small, and indicated that the electronic nature and steric effects of the ligand greatly affect the coordination state of the boron atom.

The S_N2 reaction is a fundamental organic reaction. In the transition state, the central carbon atom forms a three-center four-electron bond, which is called a hypervalent bond. For the main group elements below the third row in the periodic table, such as silicon, phosphorus, sulfur, and iodine, hypervalent compounds are quite familiar. In contrast, it was long believed that second row elements, such as carbon and boron, were unable to form stable hypervalent compounds.

Recently, we developed a sterically rigid anthracene-based tridentate ligand and characterized the stable hypervalent carbon compound **1**[1] and boron compounds **2**[1b,2] by X-ray crystallographic analyses and density functional theory (DFT) calculations (Figure 1). The C–O and B–O distances were considerably shorter than the sum of the van der Waals radii. In addition, we found bond paths between the C–O and B–O bonds by Atoms-In-Molecules (AIM) analyses.[3] These observations indicated that these compounds took a hypervalent state although the attractive interactions are weak. We then prepared hypervalent carbon species **3**[4] and boron species **4**[5] using a flexible van Koten type tridentate ligand (Figure 1). Although longer C–O (or B–O) distances were observed in **3** or **4** compared to those for the anthracene compound **1** or **2**, the X-ray electron-density analyses and DFT calculations supported the fact that these compound **3** or **4** were also hypervalent species.

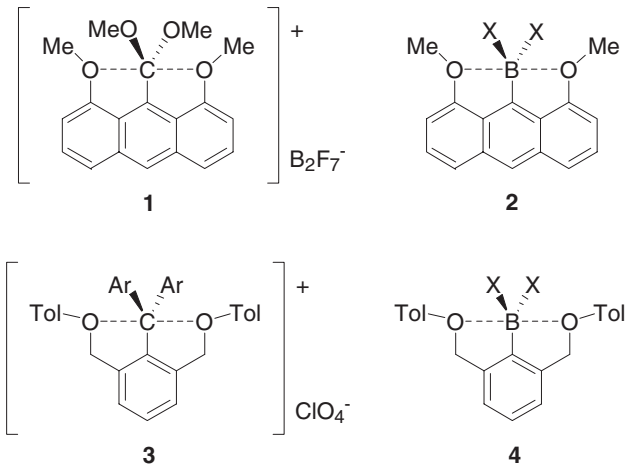

1 **2** **3** **4**

Figure 1. Pentacoordinate carbon and boron compounds.

During the course of our study, we found that some of the carbon and boron compounds were not hypervalent compounds, but instead had a preferred tetracoordinate structure in which one of the two coordinating atoms interacts with the central atom. The coordination state depends on the substituents on the central atom and the ligand itself. One such example is shown in Figure 2. The results show that when the boron atom becomes more electrophilic as in **2a**, or the donor groups become more nucleophilic as in **2c**, the coordination state tends to be tetracoordinate.[2,6] These two cases prefer forming one strong bond rather than two weak bonds.

In the flexible ligand series, the B–O distances apparently depend on the substituents on the central boron atom (Figure 3). Especially **4a**, which has the weakest electrophilicity of the central boron atoms in this series, is concluded to be a tricoordinate based on the long B–O distances (3.024(3) and 3.155(3) Å) in comparison to the other pentacoordinate boron species.

In addition, the difference in B–O distances between **2b** (Figure 2) and **4b** (Figure 3) clearly shows that the steric rigidity of the tridentate ligand plays an important role in the strength of the hypervalent bonding interaction. Recently, we reported that the sterically rigid acridinium tridentate ligand is

Published on the web June 30, 2010; doi:10.1246/bcsj.20090342

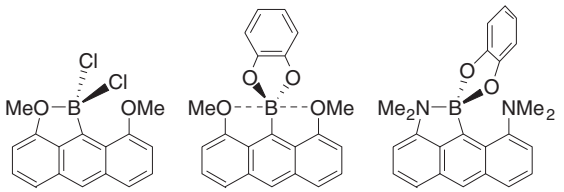

2a **2b** **2c**

	B-O distance/Å	coordination state
2a	1.686(7), 2.790(7)	tetracoordinate
2b	2.379(2), 2.441(2)	pentacoordinate
2c	1.809(2), 2.941(2)	tetracoordinate

Figure 2. The boron compounds bearing an anthracene-based tridentate ligand.

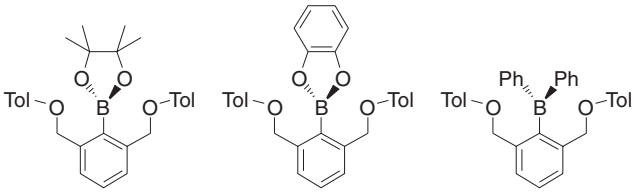

4a **4b** **4c**

	B-O distance/Å	coordination state
4a	3.024(3), 3.155(3)	tricoordinate
4b	2.528(9), 2.660(9) (1st) 2.496(9), 2.703(10) (2nd)	pentacoordinate
4c	2.561(3), 2.749(4) (1st) 2.539(3), 2.752(4) (2nd)	pentacoordinate

Figure 3. The boron compounds bearing a 2,6-bis(*p*-tolyloxymethyl)benzene ligand. For **4b** and **4c**, the B–O distances for the two independent molecules are shown.

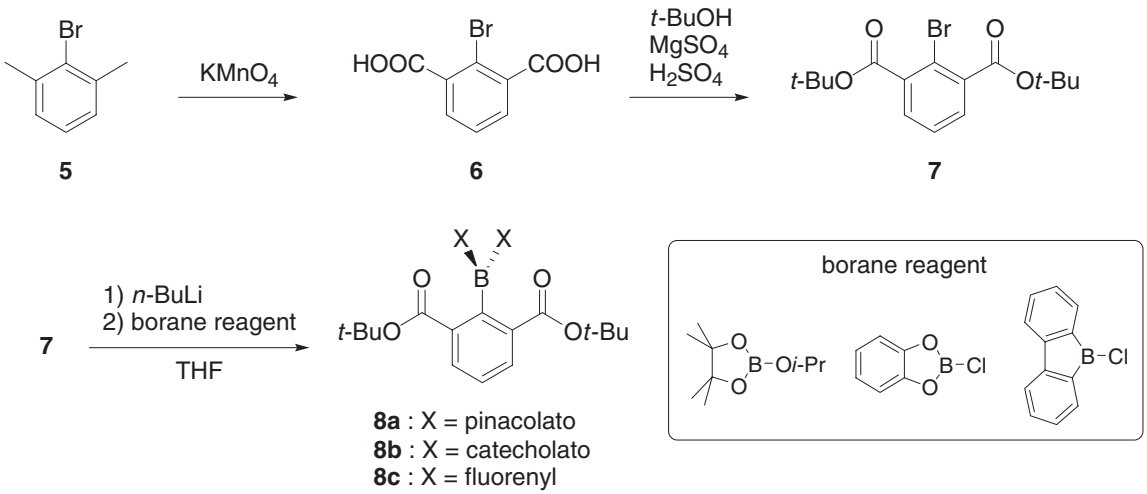

Scheme 1. Preparation of boron compounds using 2,6-bis(*t*-butoxycarbonyl)phenyl ligand.

effective for increasing the hypervalent interaction as in the anthracene ligand (B–O distances in the catechol substituent are 2.375(8) and 2.437(8) Å).[7]

On the other hand, it is expected that the donicity of the ligand also affects the coordination state, but it is not totally clarified. Because pentacoordinate boron compounds have been characterized by X-ray analysis, only with a tridentate ligand bearing two oxygen donor groups. In fact, all boron compounds bearing two dialkylamino[6,8] or alkylthio groups[4,9] as the two coordinating groups were found to have the unsymmetrical tetracoordinate structure by X-ray analysis. To investigate the influence of the coordination ability of the donor group, we focused our attention on the carbonyl ligand as the oxygen donor group.

The donicity of the carbonyl oxygen atom to the boron atom is quite complicated in order to be significantly influenced by steric factors, although it is expected that the B–O interaction should be more favorable for the carbonyl ligand than the ether ligand.[10] In the intramolecular system, however, the steric factors influencing the coordination are simpler than those in the intermolecular system. In addition, it is known that the donicity of the α,β-unsaturated carbonyl or amide group, which includes a resonance effect, is stronger than that of the ether group.[11]

We now report the preparation of organoboron compounds bearing ester and amide tridentate ligands, which is expected to strongly coordinate with the boron atom as compared to the ether ligand. In this report, we discuss the electronic and steric effects on the structures.

Results and Discussion

Preparation of Ester Ligand and of the Corresponding Organoboron Derivatives. The ester ligand precursor **7** was prepared by the oxidation[12] of commercially available 2-bromo-*m*-xylene (**5**), followed by esterification with isobutylene prepared in situ with *t*-BuOH in the presence of H_2SO_4 adsorbed on $MgSO_4$[13] (Scheme 1). The *t*-butyl ester was used as an ester ligand to avoid nucleophilic attack of the organo-

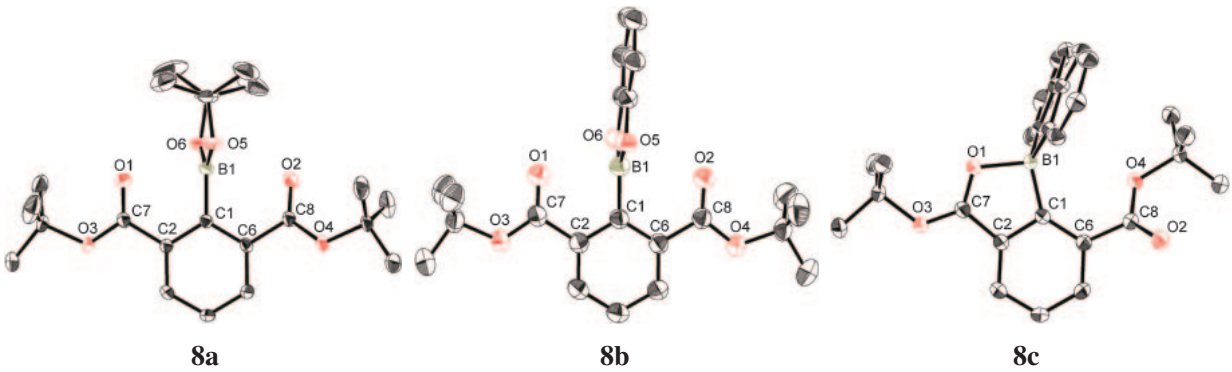

Figure 4. ORTEP drawings of **8a**, **8b**, and **8c** (50% thermal ellipsoid; all hydrogen atoms and 2-hydroxy-4,4,5,5-tetramethyl-1,3,2-dioxaborolane for **8a** are omitted for clarity).

metal reagent on the ester groups in the next step. Fortunately, halogen–metal exchange using *n*-BuLi was successful, followed by treatment with the corresponding boron reagent to give the pinacolato derivative **8a**, catecholato derivative **8b**, and fluorenyl derivative **8c** (Scheme 1).

All the derivatives of **8** are stable and can be handled in air. The ^{1}H and ^{13}C NMR spectra ($CDCl_3$) for compounds **8a**–**8c** showed a symmetric pattern for the tridentate ligands. For example, one sharp singlet signal for the *t*-Bu group (18H, δ 1.40) in the ^{1}H NMR and one carbonyl carbon signal (δ 166.4) in the ^{13}C NMR were observed in **8b**. In contrast, the ^{11}B NMR spectra of **8** showed different behavior between **8a**, **8b**, and **8c**. The ^{11}B NMR chemical shifts of **8a** (δ 31) and **8b** (δ 31) were similar to the chemical shifts of the corresponding tricoordinate borane derivatives (phenylpinacolborane: δ 26.7 in $CDCl_3$,[14] phenylcatecholborane: δ 32.1 in THF[15]). On the other hand, the ^{11}B NMR chemical shift of **8c** (δ 13) showed clearly a high-field shift compared to 9-phenyl-9-borafluorene (δ 64.5 in C_6D_6),[16] suggesting that the coordination form of **8c** might be different from those of **8a** and **8b** in solution.

X-ray Crystallographic Analyses of Organoboron Derivative Bearing Ester Ligand. The single crystals of **8b**, **8c** and co-crystal of **8a** and 2-hydroxy-4,4,5,5-tetramethyl-1,3,2-dioxaborolane suitable for X-ray analysis were obtained by recrystallization from a CH_2Cl_2/*n*-hexane solution. The ORTEP drawings of **8a**–**8c** are shown in Figure 4, and the structural parameters summarized in Table 1. The molecules of 2-hydroxy-4,4,5,5-tetramethyl-1,3,2-dioxaborolane that co-crystallized with **8a** are not shown because the hydroxyborane has little influence on the structure of **8a** (B1–O5: 1.359(2) Å, B1–O6: 1.372(2) Å), although a hydrogen bond between the hydroxy group of the hydroxyborane and O6 atom of **8a** exists.

The structures of **8a** and **8b** are almost symmetric, and the sum of the bond angles around the boron atom is almost 360°. The B1–O1 and B1–O2 distances of **8a** (2.524(2) and 2.570(2) Å) and **8b** (2.458(3) and 2.560(4) Å) are shorter than the sum of the van der Waals radii (3.48 Å),[17] which can be regarded as a pentacoordinated. The B–O distance average of **8b** (av. 2.51 Å) is shorter than that of **8a** (av. 2.55 Å), indicating that the degree of the B–O interactions of **8b** is stronger than that of **8a** if the B–O interactions exist. This could be due to the difference in the electronic nature on the central boron atom, i.e., the pinacolato group of **8a** is less electron-withdrawing than the catecholato group of **8b**, and the electrophilicity of the central boron atom of **8a** is reduced relative to that of **8b**.

Table 1. Selected Structural Parameters for **8a**, **8b**, and **8c**

	8a	**8b**	**8c**
Bond distance/Å			
B1–O1	2.524(2)	2.458(3)	1.634(2)
B1–O2	2.570(2)	2.560(4)	4.449(2)
B1–O4	—	—	3.105(2)
C7–O1	1.209(2)	1.211(2)	1.259(2)
C8–O2	1.206(2)	1.211(2)	1.206(2)
Bond angle/°			
O1–B1–O2	163.5(1)	165.2(1)	140.1(1)
O1–B1–O4	—	—	163.9(1)
C1–C2–C7	116.8(1)	116.6(1)	108.0(1)
C1–C6–C8	117.3(1)	118.0(1)	123.3(1)
C2–C7–O1	121.5(1)	121.4(1)	115.2(1)
C6–C8–O2	120.6(2)	122.7(1)	122.0(1)

In contrast to the other two compounds, the fluorenyl derivative **8c** clearly has an asymmetric structure in the crystal state, and only one of the carbonyl oxygen atoms is coordinated with the central boron atom. In addition, the other *t*-butyl ester group turns round, and the CH–π interactions between the *t*-butyl group and the fluorenyl ring are found based on the AIM analysis.[3] The shorter B–O distance is 1.634(2) Å and the longer distance is 3.105(2) Å. The C7–O1 length (1.259(2) Å) is longer than the C8–O2 length (1.206(2) Å) and C=O lengths of **8a** (1.206(2) and 1.209(2) Å) and **8b** (1.211(2) and 1.211(2) Å). This could be due to the effect of the resonance structure B^{-}–O–C^{+}. These results clearly indicate that the boron atom of **8c** is tetracoordinated, and explains the higher-field shifted ^{11}B NMR chemical shift in solution. This could be due to the strong electrophilicity of the boron atom of the fluorenyl derivative, and is consistent with the previous trend[2,6] that the strongly electrophilic central atom tends to take a tetracoordinate structure instead of pentacoordinate.

Preparation of Amide Ligand and the Corresponding Organoboron Derivatives. The amide ligand precursors were prepared as shown in Scheme 2. 2-Bromoisophthaloyl dichloride (**9**)[18] was treated with dimethylamine or diisopropylamine

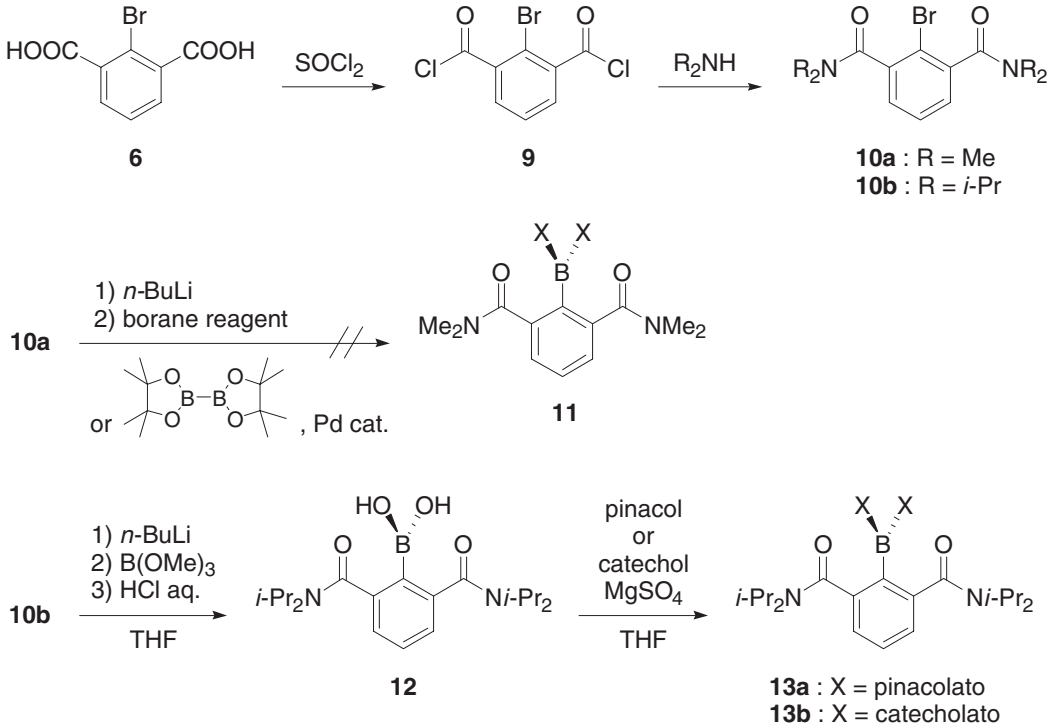

Scheme 2. Preparation of boron compounds using 2,6-bis(*N*,*N*-diisopropylaminocarbonyl)phenyl ligand.

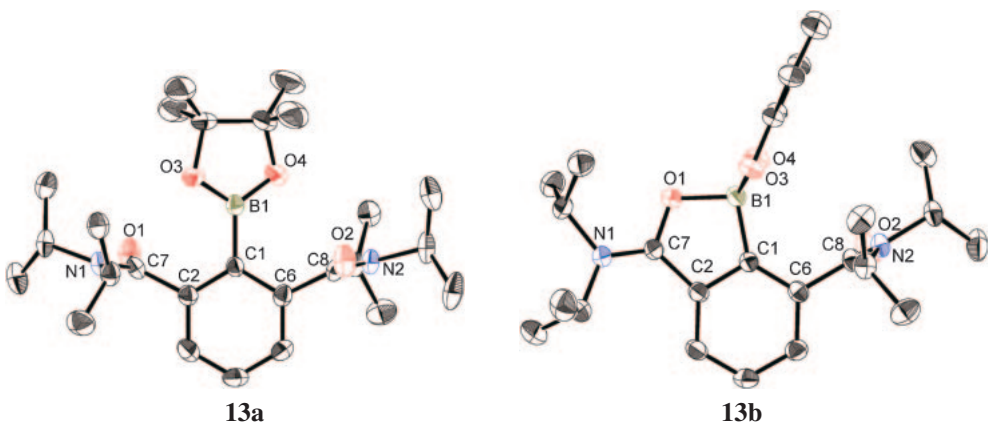

Figure 5. ORTEP drawings of **13a** and **13b** (50% thermal ellipsoid; all hydrogen atoms and water for **13b** are omitted for clarify).

to give the amide ligand precursors **10a** and **10b**, respectively. Although the lithiation of **10** was accomplished by treatment with *n*-BuLi in THF, the lithiated compound of **10a** did not react with any boron reagent due to its low solubility. In contrast, the lithiated compound of **10b** was soluble and produced boronic acid **12** after treatment with $B(OMe)_3$, then 10% HCl aqueous solution. The boronic acid **12** was condensed with catechol or pinacol in the presence of $MgSO_4$ to give the pinacolato derivative **13a** and catecholato derivative **13b**, respectively (Scheme 2). We also attempted to introduce a boron atom into **10a** by coupling reaction,[13] but it was not successful. Although all the derivatives of **13** are stable in air, the pinacolato derivative **13a** is slightly sensitive to water and is slowly hydrolyzed in solvent.

The ^{1}H and ^{13}C NMR spectra ($CDCl_3$) for compounds **13** also showed a symmetric pattern for the tridentate ligands which is similar to those of the corresponding ester derivatives **8**. In contrast, the ^{11}B NMR spectra of **13** showed different behavior between **13a** and **13b**. The ^{11}B NMR chemical shift of **13a** (δ 31) was similar to the chemical shift of the corresponding tricoordinate borane derivative (phenylpinacolborane: δ 26.7 in $CDCl_3$). On the other hand, the ^{11}B NMR chemical shift of **13b** (δ 14) clearly shows a high-field shift compared to the phenylcatecholborane (δ 32.1 in THF) and ester derivative **8b** (δ 31).

X-ray Crystallographic Analyses of Organoboron Derivative Bearing Amide Ligand. The single crystals of **13a** and **13b** suitable for X-ray analysis were obtained by recrystallization from a CH_2Cl_2/*n*-hexane solution. The ORTEP drawings of **13a** and **13b** are shown in Figure 5, and the structural parameters summarized in Table 2. The molecules of water that co-crystallized with **13b** are not shown.

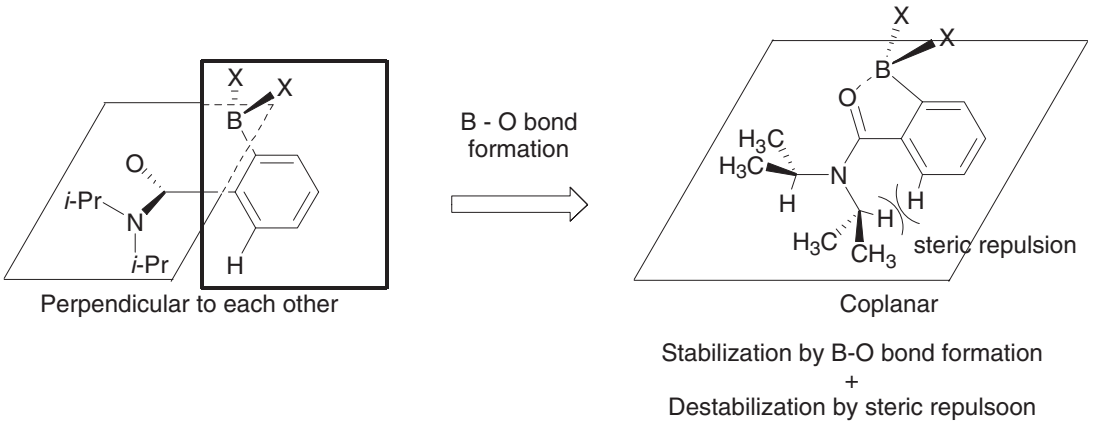

Figure 6. Steric repulsion between diisopropylamide group and benzene ring.

Table 2. Selected Structural Parameters for **13a** and **13b**

	13a	**13b**
Bond distance/Å		
B1–O1 (Å)	3.421(4)	1.561(4)
B1–O2 (Å)	3.477(4)	3.770(5)
Bond angle/°		
O1–B1–O2 (°)	134.8(1)	—

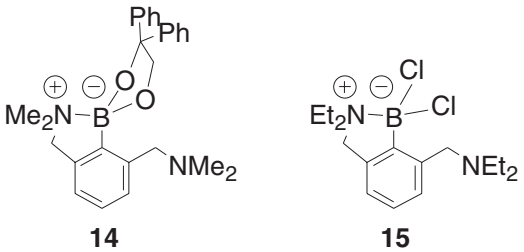

Figure 7. Structures of **14** and **15**.

In contrast to the ester ligand cases, no pentacoordinate species were found in the amide series. Although the pinacolato derivative **13a** is almost a symmetric structure like the ester ligand **8a**, both carbonyl oxygen atoms do not coordinate with the central boron atom (3.421(4) and 3.477(4) Å). This indicates that the boron atom of the pinacolato derivative **13a** is in a tricoordinated state like **4a**, which bears a flexible ether ligand (B–O bond length: 3.024(3) and 3.155(3) Å). On the other hand, the catecholato derivative **13b**, unlike the ester ligand **8b**, has an asymmetric structure and only one of the carbonyl oxygen atoms is coordinated with the central boron atom, in which the shorter B–O length is 1.561(4) Å and the longer length is 3.770(5) Å. This is consistent with the high-field shift of the ^{11}B NMR chemical shift of **13b** and clearly indicates that the boron atom of **13b** is in the tetracoordinated state.

The difference in the coordination state between the ester ligand and the amide series could be explained by the electronic and steric effects of the diisopropylamide ligand. That is, if the carbonyl oxygen atom is coordinated to the boron atom, steric repulsion occurs between the isopropyl group and aromatic proton (Figure 6) in the amide series. Thus, the less electrophilic pinacolato derivative **13a** when compared to catecholato group of **13b** prefers the tricoordinated state without coordination toward the central boron. However, the catecholato group is more electrophilic, giving rise to coordination of one of the carbonyl oxygen atoms to the central boron atom. The crystal structure of the catechol ester of the 2-(diisopropylaminocarbonyl)phenylboronic acid shows an internal coordination bond between the carbonyl oxygen atom and the boron atom[19] unlike the pinacol ester which shows the carbonyl oxygen atom far away from the boron atom.[20] However, the sum of the stabilizing energy by the formation of one strong B–O bond (covalent bond) and destabilizing energy by steric repulsion between the isopropyl group and aromatic proton overrides the sum of the stabilizing energy by the formation of two weak B–O bonds (hypervalent bond) and destabilizing energy by two steric repulsions between the isopropyl group and aromatic proton, resulting in the boron atom being in a tetracoordinated state.

Observation of B–O Bond Switching. As already described above, the X-ray crystal structure showed that the boron atoms of **8c** and **13b** are in a tetracoordinated state even though the ^{1}H and ^{13}C NMR spectra ($CDCl_3$) showed a symmetric pattern for the tridentate ligands. Therefore, ^{1}H NMR spectra of the tetracoordinate organoboron compounds **8c** and **13b** were measured at various temperatures for observation of the dynamic behavior in solutions.

In **8c**, the two *t*-Bu groups were magnetically equivalent even though the temperature was decreased to −80 °C in CD_2Cl_2. It was similar to the behavior of the N–B bond switching observed in **2a**[6] and **14** (Figure 7),[8] and this indicates that rapid B–O bond-switching take place, i.e., the difference in energies between the pentacoordinate state and tetracoordinate state is very small (Figure 8).

In contrast to **8c**, although two CH_3 signals and two CH signals (*s-cis*- and *s-trans*-isopropyl group) were observed at room temperature in **13b**, these signals in **13b** decoalesced as the temperature was lowered and finally separated into four CH_3 signals and four CH signals at −70 °C in CD_2Cl_2 (Figure 9). The energy barrier to the B–O bond-switching is estimated to be ca. 9.0 kcal mol^{-1}. In general, such B-donor

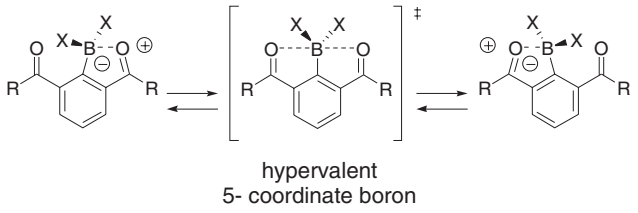

energy barrier of the B-O bond switching process

8c : not detected (at -80 °C)
13b : 9.0 kcal/mol

Figure 8. B–N bond switching equilibium in **8c** and **13b**.

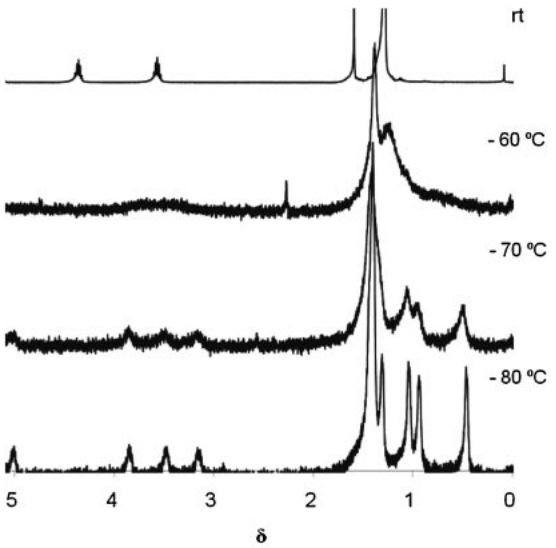

Figure 9. Variable-temperature ^{1}H NMR (CD_2Cl_2) spectra of **13b**.

bond-switching was observed only in **15**[21] which has a strongly Lewis acidic central boron atom and more donative ligand. However, despite the fact that the electronic contribution of the boron atom and ligand is small, bond switching was observed in **13b**. This could be also due to steric repulsion between the diisopropylamide ligand and aromatic proton. As you can see in the X-ray crystal structure of **13b**, the noncoordinated carbonyl plane is perpendicular to the central benzene ring plane in order to avoid steric repulsion. If bond-switching takes place, the noncoordinated carbonyl group and the central benzene ring must lie in the same plane. Thus, the pentacoordinate state is destabilized, and the energy barrier to the B–O bond-switching is increased enough to measure.

Structural Optimization and Electron-Density Distribution Study in Ester Ligand Systems by Density Functional Calculation. In order to study the nature of the interaction between the central boron atom and the two carbonyl oxygen atoms, the structures of **8a**–**8c** were optimized by the hybrid density functional theory (DFT) at the B3PW91/6-31G(d) level[22] using the Gaussian 03 program[23] (Figure 10).

In the ester systems, the optimized geometry of **8a** and **8b** are symmetric and similar to the experimental structure although the two B–O bond lengths are slightly longer than the experimental data (**8a**: calculated distance: 2.603 Å, average of experimental data: 2.55 Å, **8b**: calculated distance: 2.524 Å, average of experimental data: 2.51 Å). It should be noted that bond paths are found between the central boron atom and the two carbonyl oxygen atoms in both cases.[5] These results indicate that attractive B–O interactions are present in **8a** and **8b**. In **8b**, the small electron density ($\rho(r)$, 0.021 e/a_0^3) and the small positive Laplacian ($\nabla^2\rho(r)$, 0.050 e/a_0^5) value at the bond critical point indicate that the bond is weak and ionic. These values are similar to the values for the B–O bond in the anthracene skeleton system of **2b** ($\rho(r)$, 0.022 e/a_0^3; $\nabla^2\rho(r)$, 0.058 e/a_0^5) although the Laplacian value is slightly low. In **8a**, although the electron density and Laplacian value at the bond critical points show the same tendency for **8b**, both values are smaller than those of **8b** ($\rho(r)$, 0.017 e/a_0^3; $\nabla^2\rho(r)$, 0.046 e/a_0^5).

On the other hand, **8c** displayed a tetracoordinate structure that was found to be a global minimum, and had a pentacoordinate structure like TS. The tetracoordinate structure was only 3.5 kcal mol^{-1} more stable at the B3PW91/6-31G(d) levels including the zero-point energy (scaling factor = 0.978)[24] than the pentacoordinated one, and this corresponds with the VT NMR study. In the TS structure of **8c**, the two B–O bond lengths are nearly identical (2.380 and 2.381 Å) and shorter than in **8a** and **8b**. In addition, the electron density and Laplacian value at the bond critical points ($\rho(r)$, 0.025 e/a_0^3; $\nabla^2\rho(r)$, 0.057 e/a_0^5) are greater than those of **8a** and **8b**. It is indicated that the more electrophilic boron atom prefers the stronger B–O interactions. However, when the donicity of the oxygen atoms and electrophilicity of the boron atom are too strong, the boron atom prefers the tetracoordinated state over the pentacoordinated state.

Comparison of the Nature of Hypervalent Bond Difference in a Ligand. The structural parameters of the pentacoordinate boron compound bearing a catecholato group on the central boron atom, which is described in this paper and already been synthesized, are summarized in Figure 11.

The coordination state and the degree of B–O interaction depend on not only the substituents on the central boron atom, but also on the donicity of the ligand as indicated by the B–O bond length that is clearly shorter in the ester ligand system **8b** than in the ether ligand system **4b**. However, the sterically rigid ether ligand system **2b** has even shorter B–O distances than **8b**, which suggests that the steric rigidity of the tridentate ligand plays an important role in the hypervalent bond interaction.

Conclusion

In conclusion, organoboron compounds bearing ester **8a**–**8c** and amide **13a** and **13b** tridentate ligands were prepared and characterized by X-ray analysis. In these series, the coordination state and the degree of B–O interaction depend on the substituents on the central boron atom and the ligands. On the other hand, the VT NMR study and the DFT calculations reveal that the energy difference between the tetracoordinate and pentacoordinate structure is small. The carbonyl donating tridentate ligands prepared lead to formation of more strongly coordinating pentacoordinate boron in comparison with the corresponding ether ligand.

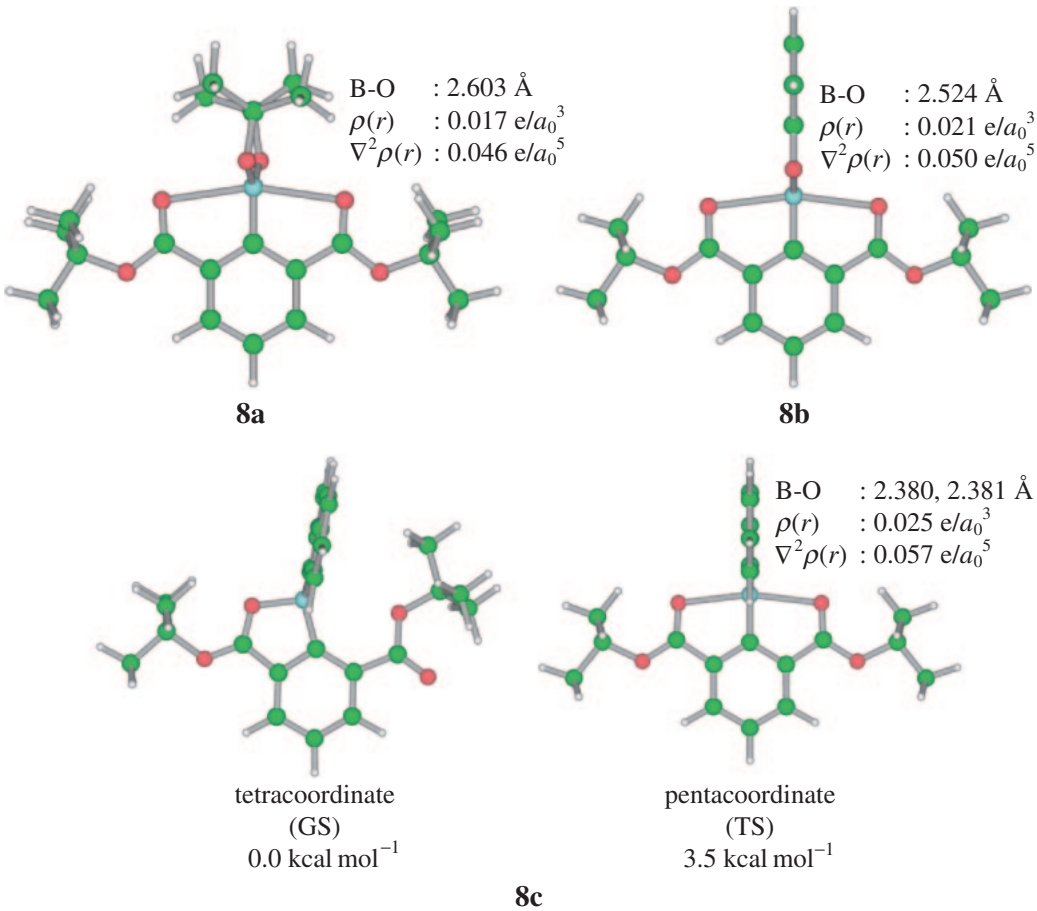

Figure 10. Optimized structures and the AIM data of **8a**–**8c** at the B3PW91/6-31G(d) level.

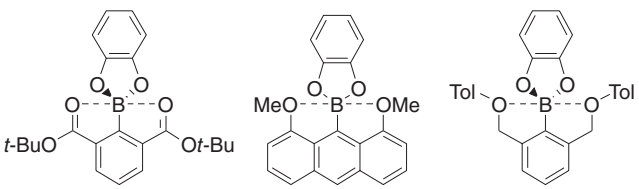

8b **2b** **4b**

	B-O distance/Å	distance ave./Å
8b	2.458(2), 2.560(2)	2.51
2b	2.379(2), 2.441(2)	2.41
4b	2.528(9), 2.660(9) (1st) 2.496(9), 2.703(10) (2nd)	2.60

Figure 11. Comparison of pentacoordinate boron compounds bearing a catecholato group on the central boron atom.

Experimental

General. The melting points were measured using a Yanaco micro melting point apparatus. The ^{1}H NMR (400 MHz), ^{11}B NMR (127 MHz), and ^{13}C NMR (100 MHz) were recorded using a JEOL EX-400 or a JEOL AL-400 spectrometer. The ^{1}H NMR chemical shifts (δ) are given in ppm downfield from Me_4Si, determined by residual chloroform (δ 7.26). The ^{11}B NMR chemical shifts (δ) are given in ppm downfield from external $BF_3 \cdot OEt_2$. The ^{13}C NMR chemical shifts (δ) are given in ppm downfield from Me_4Si, determined by $CDCl_3$ (δ 77.0). The elemental analyses were performed using a Perkin-Elmer 2400 CHN elemental analyzer. Tetrahydrofuran (THF) and benzene were freshly distilled from Na–benzophenone, and CH_2Cl_2 was distilled from CaH_2. 2-Bromoisophthalic acid (**6**),[12] 9-chloro-9-borafluorene,[25] and 2-bromoisophthaloyl dichloride (**9**)[18] were prepared by literature methods.

Synthesis of Di-*t*-butyl 2-Bromoisophthalate (7). To a suspension of anhydrous $MgSO_4$ (9.62 g, 80 mmol) in 80 mL of CH_2Cl_2, concd H_2SO_4 (1.1 mL, 20 mmol) was added under Ar. After the mixture was stirred for 15 min, 2-bromoisophthalic acid (**6**) (2.45 g, 10.0 mmol) and *t*-BuOH (10 mL, 102 mmol) were then added. The bottle containing the mixture was tightly sealed and stirred for 24 h at room temperature. The reaction mixture was then quenched with sat. $NaHCO_3$ aq. and extracted with CH_2Cl_2. The organic layer was washed with brine, and dried over $MgSO_4$. After solvent removal by evaporation, **7** (3.18 g, 8.91 mmol, y. 89%) was obtained as a colorless oil; ^{1}H NMR ($CDCl_3$, 400 MHz): δ 1.61 (s, 18H), 7.36 (t, 1H, $J = 7.6$ Hz), 7.56 (d, 2H, $J = 7.6$ Hz); ^{13}C NMR ($CDCl_3$, 100 MHz): δ 28.2, 83.0, 117.6, 126.8, 130.8, 136.9, 165.8.

Synthesis of Di-*t*-butyl 2-(4,4,5,5-Tetramethyl-1,3,2-di-

oxaborolan-2-yl)isophthalate (8a). To a THF (1 mL) solution of **7** (71 mg, 0.20 mmol), *n*-BuLi (0.14 mL, 1.58 M in hexane, 0.22 mmol) was dropwise added at −78 °C under Ar, and the mixture was stirred for 1 h. To the reaction mixture, THF (3 mL) solution of 2-isopropoxy-4,4,5,5-tetramethyl-1,3,2-dioxaborolane (0.10 mL, 0.50 mmol) was dropwise added at −78 °C. The mixture was then slowly warmed to room temperature within 15 h. The mixture was extracted with CH_2Cl_2, and the organic layer was dried over Na_2SO_4. After removal of the solvents by evaporation, co-crystals of **8a** and 2-hydroxy-4,4,5,5-tetramethyl-1,3,2-dioxaborolane suitable for X-ray analysis (100 mg, 91%) were obtained by recrystallization from *n*-hexane/CH_2Cl_2. The co-crystals were dissolved in CH_2Cl_2 and washed with H_2O several times, then dried over Na_2SO_4. After removal of the solvents by evaporation, analytically pure **8a**·0.5H_2O was obtained; mp 82.5–84.0 °C (dec); ^{1}H NMR ($CDCl_3$, 400 MHz): δ 1.48 (s, 12H), 1.57 (s, 18H), 7.37 (t, 1H, J = 7.6 Hz), 7.99 (d, 2H, J = 7.6 Hz); ^{11}B NMR ($CDCl_3$, 127 MHz): δ 30.5; ^{13}C NMR ($CDCl_3$, 100 MHz): δ 25.7, 28.1, 81.2, 83.7, 128.1, 132.0, 136.7, 166.1, the *ipso*-carbon bonded to the central boron atom was not observed; Anal. Calcd for $C_{22}H_{33}BO_6 + 0.5H_2O$: C, 63.93; H, 8.29%. Found: C, 64.14; H, 8.04%.

Synthesis of Di-*t*-butyl 2-(Benzo-1,3,2-dioxaborolan-2-yl)isophthalate (8b). To a THF (1 mL) solution of **7** (71 mg, 0.20 mmol), *n*-BuLi (0.14 mL, 1.58 M in hexane, 0.22 mmol) was dropwise added at −78 °C under Ar, and the mixture was stirred for 1 h. To the reaction mixture, THF (3 mL) solution of chlorocatecholborane (31 mg, 0.20 mmol) was dropwise added at −78 °C. The mixture was then warmed to 0 °C and stirred for 4 h. The mixture was extracted with Et_2O, and the organic layer was washed with brine and dried over Na_2SO_4. After removal of the solvents by evaporation, compound **8b** was obtained as a white solid (68 mg, 0.15 mmol, 77%). Colorless crystals of **8b** suitable for X-ray analysis were obtained by recrystallization from *n*-hexane/CH_2Cl_2; mp 158.0–159.0 °C (dec); ^{1}H NMR ($CDCl_3$, 400 MHz): δ 1.40 (s, 18H), 7.07–7.09 (m, 2H), 7.21–7.24 (m, 2H), 7.59 (t, 1H, J = 8.0 Hz), 8.19 (d, 2H, J = 8.0 Hz); ^{11}B NMR ($CDCl_3$, 127 MHz): δ 31.4; ^{13}C NMR ($CDCl_3$, 100 MHz): δ 28.0, 82.9, 112.0, 121.6, 129.5, 132.7, 136.6, 149.2, 166.4, the *ipso*-carbon bonded to the central boron atom was not observed; Anal. Calcd for $C_{22}H_{25}BO_6$: C, 66.69; H, 6.36%. Found: C, 66.66; H, 6.56%.

Synthesis of Di-*t*-butyl 2-(5*H*-Dibenzoborol-5-yl)isophthalate (8c). To a THF (3 mL) solution of **7** (350 mg, 1.00 mmol), *n*-BuLi (0.63 mL, 1.58 M in hexane, 1.00 mmol) was dropwise added at −78 °C under Ar, and the mixture was stirred for 1 h. To the reaction mixture, a THF (10 mL) solution of 9-chloro-9-borafluorene (198 mg, 1.00 mmol) was dropwise added at −78 °C. The mixture was then slowly warmed to room temperature within 15 h. The mixture was extracted with Et_2O, and the organic layer was washed with brine and dried over Na_2SO_4. After removal of the solvents by evaporation, the crude product was purified by column chromatography (CH_2Cl_2–*n*-hexane = 1:1) to give compound **8c** as a white solid (194 mg, 0.440 mmol, 44%). Colorless crystals of **8c** suitable for X-ray analysis were obtained by recrystallization from *n*-hexane/CH_2Cl_2; mp >300 °C; ^{1}H NMR ($CDCl_3$, 400 MHz): δ 1.26 (s, 18H), 6.92 (d, 2H, J = 7.2 Hz), 7.00 (t, 2H, J = 7.2 Hz), 7.23 (t, 2H, J = 7.2 Hz), 7.51 (t, 1H, J = 8.0 Hz), 7.64 (d, 2H, J = 7.2 Hz), 8.08 (d, 2H, J = 8.0 Hz); ^{11}B NMR ($CDCl_3$, 127 MHz): δ 13.1; ^{13}C NMR ($CDCl_3$, 100 MHz): δ 27.7, 86.4, 119.1, 126.3, 127.0, 127.4, 129.4, 132.1, 134.0, 151.0, 173.2, the two *ipso*-carbons bonded to the central boron atom were not observed; Anal. Calcd for $C_{28}H_{29}BO_4$: C, 76.37; H, 6.64%. Found: C, 76.25; H, 6.37%.

Synthesis of *N*,*N*,*N*′,*N*′-Tetraisopropyl-2-bromoisophthalamide (10b). To a CH_2Cl_2 (5 mL) solution of 2-bromoisophthaloyl dichloride (**9**) (253 mg, 1.00 mmol), diisopropylamine (0.60 mL, 4.0 mmol) was slowly added at 0 °C. The mixture was stirred overnight at room temperature. The mixture was then extracted with CH_2Cl_2, and the organic layer was washed with brine and dried over $MgSO_4$. After removal of the solvents by evaporation, the crude product was purified by column chromatography (AcOEt–MeOH = 20:1) to give compound **10b** as a white solid (378 mg, 0.919 mmol, 92%); mp 220.5–221.0 °C; ^{1}H NMR ($CDCl_3$, 400 MHz): δ 1.03 (d, 12H, J = 6.8 Hz), 1.22 (d, 12H, J = 6.8 Hz), 3.53 (sep, 2H, J = 6.8 Hz), 3.62 (sep, 2H, J = 6.8 Hz), 7.13 (d, 2H, J = 7.6 Hz), 7.35 (t, 1H, J = 7.6 Hz); ^{13}C NMR ($CDCl_3$, 100 MHz): δ 20.0, 20.6, 46.0, 51.2, 115.2, 126.0, 128.1, 141.1, 167.8; Anal. Calcd for $C_{20}H_{31}BrN_2O_2$: C, 58.39; H, 7.60; N, 6.81%. Found: C, 58.72; H, 7.88; N, 6.74%.

Synthesis of *N*,*N*,*N*′,*N*′-Tetraisopropyl-2-(dihydroxyboryl)isophthalamide (12). To a THF (15 mL) solution of **10b** (206 mg, 0.50 mmol), *n*-BuLi (0.32 mL, 1.58 M in hexane, 0.50 mmol) was dropwise added at −78 °C under Ar, and the mixture was stirred for 1 h. To the reaction mixture, trimethyl borate (0.10 mL, 0.90 mmol) was dropwise added at −78 °C and stirred for 3 h at the same temperature. The mixture was slowly warmed to room temperature within 15 h. To the reaction mixture, 10% HCl aq. was added and the mixture was stirred for 1 h. The mixture was extracted with CH_2Cl_2, and the organic layer was washed with brine and dried over Na_2SO_4. After removal of the solvents by evaporation, compound **12** was obtained as a white solid (179 mg, 0.476 mmol, 95%). The crude product of **12** was used without further purification.

Synthesis of *N*,*N*,*N*′,*N*′-Tetraisopropyl-2-(4,4,5,5-tetramethyl-1,3,2-dioxaborol-2-yl)isophthalamide (13a). A mixture of **12** (92 mg, 0.24 mmol), pinacol (29 mg, 0.25 mmol), and anhydrous $MgSO_4$ (100 mg) in THF (6 mL) was refluxed for 15 h under N_2. After the mixture was filtered to remove the solid materials, the solvents were removed by evaporation. The crude product was recrystallized from dry *n*-hexane/CH_2Cl_2 to afford compound **13a** as colorless crystals suitable for X-ray analysis (71 mg, 0.156 mmol, 65%); mp 223.0–234.0 °C; ^{1}H NMR ($CDCl_3$, 400 MHz): δ 1.12 (d, 12H, J = 6.8 Hz), 1.27 (s, 12H), 1.54 (d, 12H, J = 6.8 Hz), 3.48 (sep, 2H, J = 6.8 Hz), 3.78 (sep, 2H, J = 6.8 Hz), 7.08 (d, 2H, J = 7.6 Hz), 7.31 (t, 1H, J = 7.6 Hz); ^{11}B NMR ($CDCl_3$, 127 MHz): δ 30.7; ^{13}C NMR ($CDCl_3$, 100 MHz): δ 20.2, 20.4, 24.6, 45.6, 51.1, 84.2, 124.0, 129.1, 145.7, 171.4, the *ipso*-carbon bonded to the central boron atom was not observed; Anal. Calcd for $C_{26}H_{43}BN_2O_4$: C, 68.12; H, 9.45; N, 6.11%. Found: C, 68.31; H, 9.27; N, 5.98%.

Synthesis of *N*,*N*,*N*′,*N*′-Tetraisopropyl-2-(benzo-1,3,2-dioxaborolan-2-yl)isophthalamide (13b). A mixture of **12**

Table 3. Crystallographic Data for **8a**, **8b**, and **8c**

	8a	**8b**	**8c**
Formula	$C_{28}H_{46}B_2O_9$	$C_{22}H_{25}BO_6$	$C_{28}H_{29}BO_4$
Molecular weight	548.27	396.23	440.32
Crystal system	monoclinic	monoclinic	triclinic
Space group	$P2_1/a$	$P2_1/c$	$P\bar{1}$
Color	colorless	colorless	colorless
Habit	plate	plate	plate
Crystal dimensions/mm^3	0.20 × 0.10 × 0.10	0.30 × 0.20 × 0.10	0.20 × 0.18 × 0.05
a/Å	11.353(2)	11.651(2)	9.155(1)
b/Å	19.817(4)	16.803(3)	9.256(2)
c/Å	14.906(4)	12.096(3)	14.137(2)
α/°	90	90	94.788(2)
β/°	109.09(1)	116.893(1)	97.861(2)
γ/°	90	90	91.648(2)
V/Å^3	3169.16(12)	2111.96(7)	1181.6(3)
Z	4	4	2
D_{calcd}/g cm^{-3}	1.149	1.246	1.238
Abs coeff/mm^{-1}	0.083	0.089	0.081
F(000)	1184	840	468
Radiation; λ/Å	Mo Kα, 0.71073	Mo Kα, 0.71073	Mo Kα, 0.71073
Temp/K	173	298	173
Data collected	$+h$, $\pm k$, $\pm l$	$+h$, $\pm k$, $\pm l$	$+h$, $\pm k$, $\pm l$
Data/restraints/param	7418/0/367	5068/0/268	4964/0/304
R_1 [$I > 2\sigma(I)$]	0.0559	0.0544	0.0468
wR_2 (all data)	0.1804	0.1722	0.1348
GOF	1.124	1.152	1.044
Solv for crystallization	*n*-hexane/CH_2Cl_2	*n*-hexane/CH_2Cl_2	*n*-hexane/CH_2Cl_2

(75 mg, 0.20 mmol), catechol (23 mg, 0.21 mmol), and anhydrous $MgSO_4$ (100 mg) in THF (6 mL) was refluxed for 15 h under N_2. After the mixture was filtered to remove the solid materials, the solvents were removed by evaporation. The crude product was dissolved in CH_2Cl_2, washed with water, and dried over anhydrous $MgSO_4$. After removal of the solvents by evaporation, the crude product was recrystallized from *n*-hexane/CH_2Cl_2 to afford compound **13b** as colorless crystals suitable for X-ray analysis (53 mg, 0.12 mmol, 59%); mp 118.0–119.5 °C (dec); ^{1}H NMR ($CDCl_3$, 400 MHz): δ 1.28 (d, 12H, J = 6.8 Hz), 1.30 (d, 12H, J = 6.8 Hz), 3.55 (sep, 2H, J = 6.8 Hz), 4.39 (sep, 2H, J = 6.8 Hz), 6.66–6.69 (m, 2H), 6.78–6.80 (m, 2H), 7.42 (t, 1H, J = 7.6 Hz), 7.53 (d, 2H, J = 7.6 Hz); ^{11}B NMR ($CDCl_3$, 127 MHz): δ 13.8; ^{13}C NMR ($CDCl_3$, 100 MHz): δ 20.1, 20.3, 48.2, 51.2, 109.7, 118.5, 127.4, 128.8, 138.3, 151.9, 170.5, the *ipso*-carbon bonded to boron was not observed; Anal. Calcd for $C_{26}H_{35}BN_2O_4 + 1H_2O$: C, 66.67; H, 7.96; N, 5.98%. Found: C, 66.59; H, 7.93; N, 5.76%.

X-ray Analysis. The X-ray data for **8a**, **8b**, and **13b** were collected on a Mac Science DIP2030 imaging plate diffractometer and irradiated with graphite monochromated Mo Kα radiation (λ = 0.71073 Å) and processed using DENZO[26] and SCALEPACK. The X-ray data for **8c** and **13a** were collected on a Bruker SMART APEXII CCD diffractometer and irradiated with graphite monochromated Mo Kα radiation (λ = 0.71073 Å) and processed using APEX program suite. The structure was solved by a direct method using the SIR-97 program.[27] Refinement on F^2 was carried out using the full-matrix least-squares by the SHELXL-97 program.[28] All non-hydrogen atoms were refined using anisotropic thermal

Table 4. Crystallographic Data for **13a** and **13b**

	13a	**13b**
Formula	$C_{26}H_{43}BN_2O_4$	$C_{26}H_{37}BN_2O_5$
Molecular weight	458.43	468.39
Crystal system	monoclinic	monoclinic
Space group	$P2_1/c$	$P2_1$
Color	colorless	colorless
Habit	plate	plate
Crystal dimensions/mm^3	0.20 × 0.10 × 0.05	0.50 × 0.20 × 0.10
a/Å	7.410(2)	13.607(5)
b/Å	21.658(5)	7.338(2)
c/Å	17.179(4)	13.590(6)
α/°	90	90
β/°	101.730(3)	103.495(1)
γ/°	90	90
V, Å^3	2699.4(10)	1319.47(8)
Z	4	2
D_{calcd}/g cm^{-3}	1.128	1.179
Abs coeff/mm^{-1}	0.074	0.080
F(000)	1000	504
Radiation; λ/Å	Mo Kα, 0.71073	Mo Kα, 0.71073
Temp/K	173	173
Data collected	$+h$, $\pm k$, $\pm l$	$+h$, $\pm k$, $\pm l$
Data/restraints/param	6113/0/310	3347/1/316
R_1 [$I > 2\sigma(I)$]	0.0736	0.0578
wR_2 (all data)	0.2282	0.1757
GOF	1.045	1.204
Solv for crystallization	*n*-hexane/CH_2Cl_2	*n*-hexane/CH_2Cl_2

parameters. In compound **13b**, the O5 atom of water is disordered and the hydrogen atoms are not found. The crystallographic data are summarized in Tables 3 and 4. Crystallographic data have been deposited with Cambridge Crystallographic Data Centre: Deposition number CCDC-759739, CCDC-759740, CCDC-759741, CCDC-759742, and CCDC-759743 for **8a**, **8b**, **8c**, **13a**, and **13b**, respectively. Copies of the data can be obtained free of charge via http://www.ccdc.cam.ac.uk/conts/retrieving.html (or from the Cambridge Crystallographic Data Centre, 12, Union Road, Cambridge, CB2 1EZ, U.K.; Fax: +44 1223 336033; e-mail: deposit@ccdc.cam.ac.uk).

References

1 a) K.-y. Akiba, M. Yamashita, Y. Yamamoto, S. Nagase, *J. Am. Chem. Soc.* **1999**, *121*, 10644. b) M. Yamashita, Y. Yamamoto, K.-y. Akiba, D. Hashizume, F. Iwasaki, N. Takagi, S. Nagase, *J. Am. Chem. Soc.* **2005**, *127*, 4354.

2 M. Yamashita, Y. Yamamoto, K.-y. Akiba, S. Nagase, *Angew. Chem., Int. Ed.* **2000**, *39*, 4055.

3 a) R. F. W. Bader, *Atoms in Molecules—A Quantum Theory*, Oxford University Press, Oxford, **1990**. b) R. F. W. Bader, *Chem. Rev.* **1991**, *91*, 893. c) R. F. W. Bader, T. S. Slee, D. Cremer, E. Kraka, *J. Am. Chem. Soc.* **1983**, *105*, 5061. d) R. F. W. Bader, *J. Phys. Chem. A* **1998**, *102*, 7314.

4 K.-y. Akiba, Y. Moriyama, M. Mizozoe, H. Inohara, T. Nishii, Y. Yamamoto, M. Minoura, D. Hashizume, F. Iwasaki, N. Takagi, K. Ishimura, S. Nagase, *J. Am. Chem. Soc.* **2005**, *127*, 5893.

5 J.-y. Nakatsuji, Y. Moriyama, S. Matsukawa, Y. Yamamoto, K.-y. Akiba, *Main Group Chem.* **2006**, *5*, 277.

6 M. Yamashita, K. Kamura, Y. Yamamoto, K.-y. Akiba, *Chem.—Eur. J.* **2002**, *8*, 2976.

7 T. Yano, T. Yamaguchi, Y. Yamamoto, *Chem. Lett.* **2009**, *38*, 794.

8 a) S. Toyota, T. Futawaka, H. Ikeda, M. Ōki, *J. Chem. Soc., Chem. Commun.* **1995**, 2499. b) S. Toyota, T. Futawaka, M. Asakura, H. Ikeda, M. Ōki, *Organometallics* **1998**, *17*, 4155.

9 S. Toyota, N. Uemitsu, M. Ōki, *Heteroat. Chem.* **2004**, *15*, 241.

10 A. Rauk, I. R. Hunt, B. A. Keay, *J. Org. Chem.* **1994**, *59*, 6808.

11 T. Toyota, M. Asakura, T. Sakaue, *Bull. Chem. Soc. Jpn.* **2002**, *75*, 2667.

12 A. Padwa, K. E. Krumpe, J. M. Kassir, *J. Org. Chem.* **1992**, *57*, 4940.

13 S. W. Wright, D. L. Hageman, A. S. Wright, L. D. McClure, *Tetrahedron Lett.* **1997**, *38*, 7345.

14 T. Ishiyama, M. Murata, N. Miyaura, *J. Org. Chem.* **1995**, *60*, 7508.

15 N. Farfán, R. Contreras, *J. Chem. Soc., Perkin Trans. 2* **1987**, 771.

16 P. E. Romero, W. E. Piers, S. A. Decker, D. Chau, T. K. Woo, M. Parvez, *Organometallics* **2003**, *22*, 1266.

17 J. A. Dean, *Lange's Handbook of Chemistry*, 11th ed., McGraw-Hill, New York, **1973**, pp. 3–119.

18 A. Bugarin, B. T. Connell, *Organometallics* **2008**, *27*, 4357.

19 X.-C. Liu, J. L. Hubbard, W. H. Scouten, *J. Organomet. Chem.* **1995**, *493*, 91.

20 S. W. Coghlan, R. L. Giles, J. A. K. Howard, L. G. F. Patrick, M. R. Probert, G. E. Smith, A. Whiting, *J. Organomet. Chem.* **2005**, *690*, 4784.

21 R. Schlengermann, R. Sieler, E. Hey-Hawkins, *Main Group Chem.* **1997**, *2*, 141.

22 a) A. D. Becke, *Phys. Rev.* **1988**, *A38*, 3098. b) A. D. Becke, *J. Chem. Phys.* **1993**, *98*, 5648. c) J. P. Perdew, Y. Wang, *Phys. Rev. B* **1992**, *45*, 13244.

23 M. J. Frisch, G. W. Trucks, H. B. Schlegel, G. E. Scuseria, M. A. Robb, J. R. Cheeseman, J. A. Montgomery, Jr., T. Vreven, K. N. Kudin, J. C. Burant, J. M. Millam, S. S. Iyengar, J. Tomasi, V. Barone, B. Mennucci, M. Cossi, G. Scalmani, N. Rega, G. A. Petersson, H. Nakatsuji, M. Hada, M. Ehara, K. Toyota, R. Fukuda, J. Hasegawa, M. Ishida, T. Nakajima, Y. Honda, O. Kitao, H. Nakai, M. Klene, X. Li, J. E. Knox, H. P. Hratchian, J. B. Cross, V. Bakken, C. Adamo, J. Jaramillo, R. Gomperts, R. E. Stratmann, O. Yazyev, A. J. Austin, R. Cammi, C. Pomelli, J. W. Ochterski, P. Y. Ayala, K. Morokuma, G. A. Voth, P. Salvador, J. J. Dannenberg, V. G. Zakrzewski, S. Dapprich, A. D. Daniels, M. C. Strain, O. Farkas, D. K. Malick, A. D. Rabuck, K. Raghavachari, J. B. Foresman, J. V. Ortiz, Q. Cui, A. G. Baboul, S. Clifford, J. Cioslowski, B. B. Stefanov, G. Liu, A. Liashenko, P. Piskorz, I. Komaromi, R. L. Martin, D. J. Fox, T. Keith, M. A. Al-Laham, C. Y. Peng, A. Nanayakkara, M. Challacombe, P. M. W. Gill, B. Johnson, W. Chen, M. W. Wong, C. Gonzalez, J. A. Pople, *Gaussian 03*, *Revision C.02*, Gaussian, Inc., Wallingford CT, **2004**.

24 J. P. Merrick, D. Moran, L. Radom, *J. Phys. Chem. A* **2007**, *111*, 11683.

25 H. Hong, T. C. Chung, *J. Organomet. Chem.* **2004**, *689*, 58.

26 Z. Otwinowski, W. Minor, *Methods Enzymol.* **1997**, *276*, 307.

27 A. Altomare, M. C. Burla, M. Camalli, G. L. Cascarano, C. Giacovazzo, A. Guagliardi, A. G. G. Moliterni, G. Polidori, R. Spagna, *J. Appl. Cryst.* **1999**, *32*, 115.

28 G. M. Sheldrick, *SHELX-97*, University of Göttingen, Göttingen, Germany, **1997**.